Complex Landau-Ginzburg theory of the hidden order in URu_2Si_2

2010 EPL 89 57006

(http://iopscience.iop.org/0295-5075/89/5/57006)

A Letters Journal Exploring the Frontiers of Physics

March 2010

EPL, **89** (2010) 57006
doi: 10.1209/0295-5075/89/57006

www.epljournal.org

Complex Landau-Ginzburg theory of the hidden order in URu_2Si_2

K. Haule[(a)] and G. Kotliar

Department of Physics, Rutgers University - Piscataway, NJ 08854, USA

received 22 December 2009; accepted in final form 26 February 2010
published online 26 March 2010

PACS 71.27.+a – Strongly correlated electron systems; heavy fermions

Abstract – We develop a Landau-Ginzburg theory of the hidden-order phase and the local moment antiferromagnetic phase of URu_2Si_2. We unify the two broken symmetries in a common complex-order parameter and derive many experimentally relevant consequences such as the topology of the phase diagram in magnetic field and pressure. The theory accounts for the appearance of a moment under application of stress and the thermal expansion anomaly across the phase transitions. It identifies the low-energy mode which is seen in the hidden-order phase near the commensurate wave vector (0, 0, 1) as the pseudo-Goldstone mode of the approximate $U(1)$ symmetry.

URu_2Si_2 is arguably the most intriguing heavy-fermion material and its electronic structure has continued to be the focus of intensive investigations. At 17.7 K, it displays a phase transition to a phase for which, in spite of a large number of experimental efforts, the order parameter has not been identified and it is therefore referred to as hidden order (HO) [1].

Recent first-principles LDA+DMFT calculations showed that in the paramagnetic phase of URu_2Si_2, the local ground state of the $5f^2$ configuration, and its first-excited state are two singlets, $|\emptyset\rangle$ and $|1\rangle$ of opposite symmetry under x and y reflection, separated by a crystal field splitting Δ.

We proposed that the order parameter of the hidden-order (HO) and local moment antiferromagnetic (LMA) phase is the excitonic mixing between the two lowest-lying configurations of the f electrons [2]. The excitonic mixing of the two singlets is described by a complex-order parameter $\langle X_{\emptyset 1}(j)\rangle = \psi_j/2 = (\psi_{1,j} + i\psi_{2,j})/2$, where $X_{\emptyset 1}(j)$ is the Hubbard operator $|\emptyset\rangle\langle 1|$ at site j. ψ_2 is proportional to the magnetization along the z-axis in the material, while ψ_1 is proportional to the hexadecapole operator $(J_xJ_y + J_yJ_x)(J_x^2 - J_y^2)$. The characteristic shape of the hexadecapole is shown in fig. 1(c). The presence of ψ_1 does not break the time reversal symmetry, nor the tetragonal symmetry, but it does break the reflection symmetry along the x- and y-axis. We identify the phase with nonzero ψ_1 as the "hidden-order" phase, and the phase with nonzero ψ_2 as the LMA phase. In this picture, the LMA and the HO order parameters are intimately connected, and they are related by an internal rotation in parameter space.

In this paper, we build on these insights from LDA + DMFT microscopic theory to construct a low-energy *phenomenological model*, and to establish contact with many of the available experimental results on this material. Phenomenological theories of the Landau Ginzburg type for URu_2Si_2 have been developed before [3–5]. However an approximate symmetry between the LMA and and the HO phase has not been noticed before, and the material specific information resulting from the microscopic calculations, was not available before. The new insights from LDA + DMFT calculation restricts the effective theory enough to result in a large number of consequences that can be compared with experiment, as for example the response of the system to pressure, uniaxial stresses and weak external magnetic field. In addition, the simplifications offered by the low-energy effective Hamiltonian of Landau-Ginzburg type allow us to obtain analytical expressions which cannot be obtained in the full LDA + DMFT solution.

We take the symmetry of the low-lying crystal field sequence from LDA+DMFT calculation $|\emptyset\rangle = \frac{i}{\sqrt{2}}(|4\rangle - |-4\rangle)$, and $|1\rangle = \frac{\cos(\phi)}{\sqrt{2}}(|4\rangle + |-4\rangle) - \sin(\phi)|0\rangle$, with $\phi \sim 0.372\pi$ and $\Delta \approx 35\,\mathrm{K}$. The value of ϕ in the "pseudo-atomic" picture used here is modified from the LDA + DMFT value $\phi \sim 0.23\pi$, to take into account renormalization from higher-lying f^2 configurations. A low-energy many-body Hamiltonian, generating this sequence of levels, is sketched in the appendix. While

(a) E-mail: haule@physics.rutgers.edu

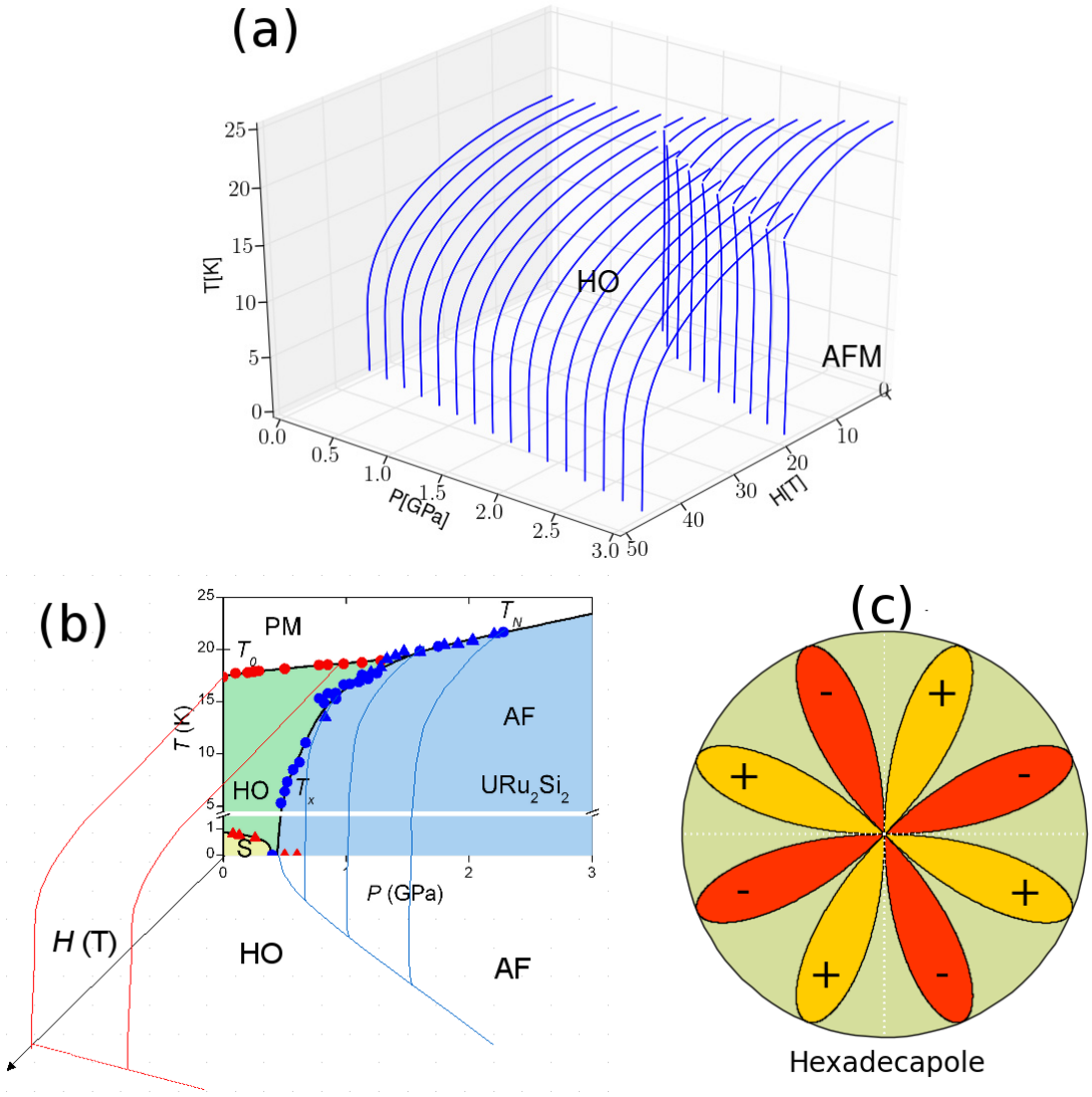

Fig. 1: (Colour on-line) (a) The phase diagram of the mean-field theory under pressure and in magnetic field. (b) Experimental phase diagram by Aoki *et al.* [11]. (c) The symmetry of the hexadecapole order parameter of the HO phase.

inspired by the earlier LDA + DMFT calculation, the Ginzburg-Landau approach is more general and could be carried out for other crystal field sequences.

It is illuminating to interpret the two low-lying configurations of the U-atom as a local two-level system of (pseudo) spins 1/2 at each lattice site. The correspondence involves the three Pauli matrices: $\sigma_3 = |\emptyset\rangle\langle\emptyset| - |1\rangle\langle 1|$, $\sigma_1 = |\emptyset\rangle\langle 1| + |1\rangle\langle\emptyset|$, $\sigma_2 = i(|1\rangle\langle\emptyset| - |\emptyset\rangle\langle 1|)$. The crystal field splitting Δ of the two singlet states plays the role of external magnetic field in the third direction, while the real and imaginary parts of the order parameter appear as the magnetization along the first and second direction in an internal order parameter space ($\langle\sigma_1\rangle = \psi_1$, $\langle\sigma_2\rangle = \psi_2$). The coupling to the external magnetic field is given by $B\mu_B(L_z + 2S_z)$ and since only the off-diagonal terms are nonzero $\langle 1|J_z|\emptyset\rangle = 4i\cos(\phi)$ and they are purely imaginary, the coupling is proportional to $|\langle 1|L_z + 2S_z|\emptyset\rangle|B\sigma_2$.

The coupling between uranium atoms is here modeled by a set of exchange constants J^α_{ij}, which we allow to be different in the two different ordered states $\alpha = 1, 2$. Ignoring for the time being the coupling to the fermionic quasiparticle excitations, the low-energy effective theory can be described by

$$H = \sum_i -\frac{\Delta}{2}\sigma^i_3 - \mu_B B|\langle 1|L_z + 2S_z|\emptyset\rangle|\sigma^i_2 + \sum_{i,j}\frac{1}{2}(J^1_{ij}\sigma^i_1\sigma^j_1 + J^2_{ij}\sigma^i_2\sigma^j_2). \quad (1)$$

This Hamiltonian should be regarded as a simplified toy model to capture symmetry-related changes not to far from the phase transitions. The LDA + DMFT treatment indicates that a more refined treatment should include the coupling to dispersing electronic excitations. This coupling

is important for understanding several properties, including the low-temperature superconductivity and the Fermi surface reconstruction as a result of the coupling of the fermions to the excitonic mode. The LDA + DMFT Fermi surface has been shown to give rise to partially nested features with a wave vector (0.6,0,0) [2]. Consequently, the itinerant electrons control the magnetic response around this wave vector as shown in ref. [6]. The analysis of the coupling of the mode to the fermionic quasiparticles is left for future study.

We now treat this Hamiltonian in the mean-field approximation and arrive at an effective free energy of the spin system, written in terms of the order parameters $\psi_{\alpha,i}$ and the conjugate Weiss fields $h_{\alpha,i}$ [7]

$$F[h,\psi]=\frac{1}{2}\sum_{ij,\alpha=(1,2)} J_{ij}^{\alpha}\,\psi_{\alpha,i}\psi_{\alpha,j}-\sum_{i,\alpha=(1,2)}(h_{\alpha,i}+b_{\alpha})\psi_{\alpha,i} -\frac{1}{2}T\sum_{i}\log\left(\cosh\left(\beta\sqrt{(\Delta/2)^2+(h_{1,i})^2+(h_{2,i})^2}\right)\right). \tag{2}$$

Here $b_2\equiv b=B\mu_B|\langle 1|L_z+2S_z|\emptyset\rangle|$, with $|\langle 1|L_z+2S_z|\emptyset\rangle|=3.2\cos(\phi)\approx 1.25$, is proportional to the external magnetic field B, while b_1 is a fictitious field which couples to the hexadecapole order. The imaginary part of ψ breaks the time reversal symmetry and therefore couples to the magnetic field. The mean-field equations can be obtained by extremizing the free energy eq. (2)

$$h_{\alpha,i}+b_{\alpha}=\sum_{j}J_{ij}^{\alpha}\psi_{\alpha,j}, \tag{3}$$

$$\psi_{\alpha,i}=-\frac{h_{\alpha,i}}{2}\frac{\tanh(\beta\lambda_i)}{\lambda_i} \tag{4}$$

with $\lambda_i=\sqrt{(\Delta/2)^2+(h_{1,i})^2+(h_{2,i})^2}$.

We take the exchange constants between uranium sites in body-centered tetragonal structure to be ferromagnetic in the same plane (RKKY is ferromagnetic at short distance), and antiferromagnetic in the c-direction, favoring the staggered order with wave vector $Q=(0,0,1)$, observed experimentally [8–10]. As a result of the close similarity of the exchange constants of the hexadecapole and the LMA order parameters, both condense at the ordering vector $Q=(0,0,1)$.

When the restriction to short-range exchange is imposed, the only combination of the exchange constants that enters the mean-field equation is $J_{eff}=4|J_1|+8J_2$, where J_1 is the nearest-neighbor ferromagnetic exchange and J_2 is the antiferromagnetic exchange in the c-direction. The critical temperature in the absence of magnetic field is then given by $T_c=\Delta/(2\mathrm{atanh}(\Delta/J_{eff}))$.

Near the transition, when the field ψ is small, the free energy acquires a simple Ginzburg-Landau form

$$F[\psi]\approx\frac{1}{2}\sum_{ij,\alpha=(1,2)}J_{ij}^{\alpha}\,\psi_{\alpha,i}\psi_{\alpha,j}+\sum_{i}\widetilde{a}\psi_i^{(2)}+u(\psi_i^{(2)})^2-b\psi_{2,i},$$

where $\psi_i^{(2)}=\sum_{\alpha}(\psi_{\alpha,i})^2$ and $\widetilde{a}=\frac{\Delta}{2}\coth(\beta\Delta/2)$, while $u=\frac{\Delta}{8}[\sinh(\beta\Delta)-\beta\Delta]\frac{\cosh^2(\beta\Delta/2)}{\sinh^4(\beta\Delta/2)}$.

We determine the effective exchange constants J_{eff} at zero pressure in such a way to reproduce the experimentally observed critical temperatures $J_{eff}^1=\frac{\Delta}{\tanh(\Delta/(2T_0))}$ and $J_{eff}^2=\frac{\Delta}{\tanh(\Delta/(2T_N))}$, where $T_0=17.7\,\mathrm{K}$ is the hidden-order transition and $T_N=15.7\,\mathrm{K}$ is the Neel temperature. The exchange constants are strain dependent and for the small compression we may use the expansion

$$J_{ij}^{\alpha}\to J_{ij}^{\alpha}(1+g_{\alpha}(\varepsilon_{xx}+\varepsilon_{yy})),$$

where ε_{xx} and ε_{yy} is the strain (compression) in the x- and y-direction. The two constants g_1 and g_2 are determined in such a way to reproduce the experimental variation of transition temperature with pressure $T_c(p)$. We take $g_1=20$, $g_2=49$.

Having determined all the parameters of the Landau-Ginzburg functional, we proceed to determine the phase diagram as a function of pressure and magnetic field, which can be directly compared to the recent experimental results of refs. [10,11].

There are two solutions of the mean-field theory, the local moment antiferromagnetic solution with nonzero staggered $\psi_{2,i}$ and vanishing $\psi_{1,i}$. The second solution has nonzero staggered $\psi_{1,i}$ but vanishing $\psi_{2,i}$, hence it shows no magnetic moment and corresponds to the hidden-order phase.

Figure 1(a) shows the phase diagram of the Ginzburg-Landau theory in the magnetic field under applied pressure and fig. 1(b) show the experimentally determined phase diagram [11]. At low pressure, with decreasing temperature, there is a second-order phase transition into the hidden-order state at temperature

$$T_0=\frac{\Delta\lambda_c}{2\mathrm{arctanh}(\Delta\lambda_c/J_{eff}^1)}$$

with

$$\lambda_c=\sqrt{1+\left(\frac{2b}{\Delta}\right)^2\left(\frac{J_{eff}^1}{J_{eff}^1+J_{eff}^2}\right)^2}.$$

At a critical field,

$$b_c=\frac{\Delta}{2}(J_{eff}^1+J_{eff}^2)\sqrt{1/\Delta^2-1/(J_{eff}^1)^2},$$

the hidden-order phase is replaced by the fully polarized paramagnetic phase.

At higher pressures, there is a second-order transition into the antiferromagnetic state at temperature

$$T_N=\frac{\Delta\sqrt{1+(2b)^2}}{2\mathrm{arctanh}(\Delta\sqrt{1+(2b)^2}/J_{eff}^2)}.$$

In this phase, the staggered magnetization at zero temperature is

$$m_{(0,0,1)}=\mu_B|\langle 1|L_z+2S_z|\emptyset\rangle|\,\sqrt{1-(\Delta/J_{eff})^2}\Big/2\sim 0.4\mu_B,$$

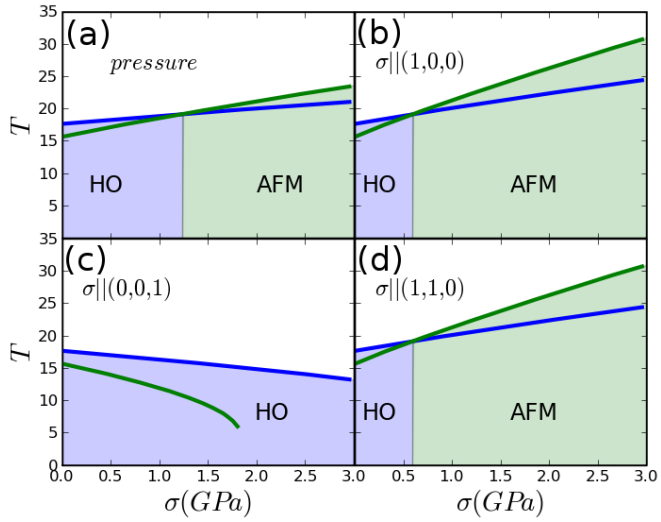

Fig. 2: (Colour on-line) The phase diagram under pressure (a) and stress (b), (d) in the *ab*-plane, and uniaxial strain (c). The critical temperatures below which the HO and the LMA solutions are possible are indicated in the diagram. The regions where LMA and HO are stable are shaded in blue and green, respectively. The transition between the HO and the LMA phase is of the first order.

in very good agreement with experiment [8]. The hidden-order phase and the antiferromagnetic phase are separated by a first-order boundary shown in fig. 1(a). It is also apparent from the figure that the magnetic field under high pressure stabilizes the hidden-order phase relatively to the antiferromagnetic phase. The hidden-order phase in a magnetic field develops a uniform magnetization directly proportional to the magnetic field $M = B\mu_B^2|\langle 1|L_z + 2S_z|\emptyset\rangle|^2|/(J^1_{eff} + J^2_{eff}) \approx 0.01\mu_B(B/T)$, in good quantitative agreement with the experiment of ref. [12]. Our model also allows us to extract the jump of the specific heat across the hidden order to paramagnetic phase boundary. It is given by

$$\Delta c_v = \left(\frac{\Delta}{T_c}\right)^3 \frac{1}{4\cosh^2\left(\frac{\Delta}{2T_c}\right)\left[\sinh(\frac{\Delta}{T_c}) - \frac{\Delta}{T_c}\right]},$$

hence $\Delta c_v/T_c \approx 245\,\mathrm{mJ/mol\,K^2}$, and is in good agreement with experiment [13].

The pressure dependence of the critical temperature is shown in fig. 2(a). A close similarity with the experiment of Hassinger *et al.* [14] is expected, since the the couplings g_1 and g_2 were optimized to reproduce the correct pressure dependence of T_c. However, the strain in *a*- and *c*-direction acts in quite an unexpected way on the stability of the two phases. The stress is connected to strain by the elastic constants ($\sigma = C\varepsilon$) (see ref. [15] for details). Their value was determined by the ultrasonic-sound-velocity measurements to be $(c_{11}, c_{33}, c_{12}, c_{13}) = (255, 313, 48, 86) \times 10^{10}\,\mathrm{erg/cm^3}$ [16].

Application of strain in the *ab*-plane ($\sigma||(1,0,0)$ or $\sigma||(1,1,0)$) destabilizes the hidden-order state, and stabilizes the antiferromagnetic state at σ around 0.6 GPa. Within our model, the transition temperatures for the two phases are given by

$$T_c^\alpha(\sigma_{xx}) = \frac{\Delta}{2}\left[\mathrm{atanh}\left(\frac{\Delta/2}{J^\alpha_{eff}(1+g_\alpha\frac{c_{33}}{(c_{11}+c_{12})c_{33}-2c_{13}^2}\sigma_{xx})}\right)\right]^{-1}$$

Hence LMA is nucleated upon application of a very small in-plane stress. This has been observed in the neutron scattering experiments of ref. [15]. In those experiments, the staggered magnetization was found to grow linearly with the applied stress, an observation which has been taken as evidence for time reversal breaking in the hidden-order phase [17]. In our framework, these measurements [15] can be interpreted as the result of inhomogeneities in the strain field, which given the very low barrier between HO and the LMA state, easily nucleates LMA regions. The LMA phase persists as a metastable state all the way to zero strain, indicating that nucleation of LMA regions is actually possible for infinitesimal stress in the presence of defects. This picture can be tested by scanning tunnelling microscopy of stressed samples.

So far, we have considered stress breaking the tetragonal symmetry. Uniaxial strain stabilizes hidden order (the T_N smaller than T_0) and decreases the hidden-order transition temperature, as shown in fig. 2(c). The formula for the two transition temperatures is given by

$$T_c^\alpha(\sigma_{zz}) = \frac{\Delta}{2}\left[\mathrm{atanh}\left(\frac{\Delta/2}{J^\alpha_{eff}(1-g_\alpha\frac{2c_{13}}{(c_{11}+c_{12})c_{33}-2c_{13}^2}\sigma_{zz})}\right)\right]^{-1}.$$

The 5.6 GPa strain leads to complete elimination of the hidden order. However, the uniaxial strain also affects the crystal field splitting Δ. We have not attempted to model this dependence quantitatively in our theory, but we notice that an increase in Δ will result in a rapid decrease of the hidden-order temperature (and the LMA critical temperature) resulting in a quantum critical point at critical value of the crystal field splitting $\Delta_c = J^1_{eff}$ separating the HO phase from the paramagnetic phase at zero temperature. This critical point may already have been accessed via Rh doping in ref. [18]. This quantum critical point is expected to be in the same universality class as that of Ising itinerant antiferromagnets [19].

To study the dilatation of the sample in the *a*- and *c*-direction due to the emergence of the HO and LMA states we add to the Landau free energy the standard elasticity terms and their coupling to the order parameter

$$\frac{1}{2}\varepsilon C\varepsilon - \varepsilon\sigma + \frac{1}{2}\sum_{ij,\alpha=(1,2)} J^\alpha_{ij}(1+g_\alpha(\varepsilon_{xx}+\varepsilon_{yy}))\,\psi_{\alpha,i}\psi_{\alpha,j}.$$

Here σ and ϵ are the stress and strain tensor and the tensor C describe the elastic moduli. Differentiating

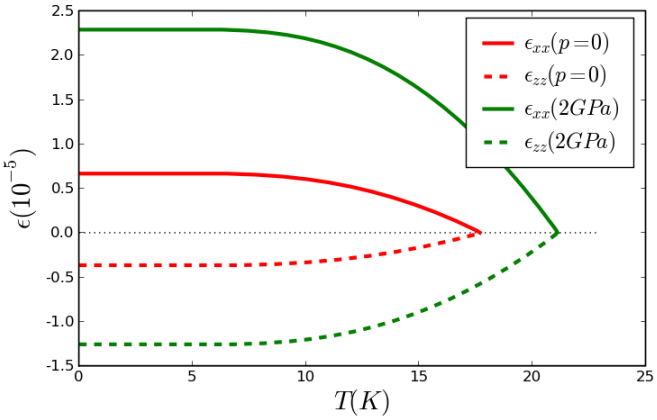

Fig. 3: (Colour on-line) The strain resulting from the phase transition into the HO and LAM state. The sample contracts in the ab-plane (positive strain), and expands in the c-direction (negative strain).

this free energy we obtain the dilatation in the a- and c-direction, $\varepsilon_{xx} = c_{33}L_\alpha/2$ and $\varepsilon_{zz} = -c_{13}L_\alpha$, where

$$L_\alpha = \frac{g_\alpha J^\alpha_{eff}(\psi_{\alpha,i})^2}{((c_{11}+c_{12})c_{33}-2c_{13}^2)}.$$

Figure 3 shows the temperature dependence of the strain in the a- and c-direction at zero pressure, where the transition into the hidden-order state occurs. The sample contracts in the ab-plane (positive strain) and expands in the c-direction (negative strain). The expansion in the c-direction is smaller than the expansion in the ab-direction. At a pressure of 2 GPa, where the LMA state is stable, the dilatation has the same trend but the magnitudes are considerably larger. Similar temperature variation of the dilatation was recently measured in ref. [20], where considerably larger dilatation was found in the transition to the LMA phase than to the hidden-order phase. This difference is connected to the larger slope of the LMA transition temperature compared to the hidden-order transition temperature.

The Landau-Ginzburg free energy explicitly exhibits a remarkable similarity between the hidden-order phase and the LMA phase. There is an approximate $U(1)$ rotational symmetry in an internal parameter space. The main difference between the two phases lies in the different values of the exchange constants, which is of the order of 6%. Our theory therefore provides a microscopic basis for the remarkable similarity between the LMA and HO phase, dubbed *adiabatic continuity* [21].

If the $U(1)$ symmetry was exact, the spontaneous breaking of this symmetry would result in a Goldstone mode describing the transverse fluctuations of the order parameter, *i.e.*, the potential would have the form of a Mexican hat with a flat bottom. Due to the small explicit breaking of the $U(1)$ symmetry, since the exchange constants J^1_{eff} and J^2_{eff} are slightly different, this Goldstone mode acquires a small mass, and we refer to it as a pseudo-Goldstone mode. In the hidden-order phase $\langle\psi_{1,i}\rangle \neq 0$ the pseudo-Goldsone mode can be identified with $\psi_{2,i}$ (the transverse fluctuation in the Mexican hat). Hence the pseudo-Goldstone mode of the hidden-order phase carries a magnetic moment and can be observed by neutron scattering. In the antiferromagnetic phase the pseudo-Goldstone mode can be identify with $\psi_{1,i}$, which carries hexadecapolar moment but no magnetic moment and is invisible to neutrons. As a result a low-lying mode at $(0,0,1)$ is only visible to neutrons in the hidden-order phase. This provides a natural explanation of the mode observed in neutron scattering experiments, as measured by Broholm *et al.* [8,9] and Villaume *et al.* [10]. The mode was observed only in the hidden-order phase, but not in the antiferromagnetic phase [10]. The energy scale of this mode is a measure of how different the hidden-order phase is from the antiferromagnetic phase, and therefore should decrease with pressure (since the difference in the exchange constants decreases with increasing pressure) and should increase with magnetic field (since the magnetic field destabilizes the antiferromagnetic phase further relative to the hidden-order phase).

In conclusion, we developed an effective theory of the paramagnetic–to–hidden-order and local antiferromagnetic transition. The theory is consistent with a large body of experimental data, is inspired by microscopic LDA + DMFT calculations, and puts URu_2Si_2 in a broader context of other f^2 systems [22,23].

* * *

We are grateful to P. Chandra, P. Coleman, and E. Hassinger for a useful discussion. We are particularly grateful to D. Aoki, E. Hassinger, and J. Flouquet for permission to reproduce their experimental phase diagram in our figure. KH was supported by Grant NFS DMR-0746395 and Alfred P. Sloan fellowship. GK was supported by NSF DMR-0906943.

Appendix

There is an extensive literature on proposed crystal field sequences for URu_2Si_2 starting with the early work of refs. [24,25]. It is usually formulated in terms of a crystal Hamiltonian with Stevens operators up to order six. Higher-order terms are not included because they would annihilate a single-particle state in the f shell, labeled by an angular momentum $l = 3$.

Inspired by the LDA+DMFT we took the two singlet states $|\emptyset\rangle = \frac{i}{\sqrt{2}}(|4\rangle - |-4\rangle)$, and $|1\rangle = \frac{\cos(\phi)}{\sqrt{2}}(|4\rangle + |-4\rangle) - \sin(\phi)|0\rangle$, as our low-lying states. They can be obtained from the following crystal field Hamiltonian:

$$H_{eff} = \widetilde{a}\left[(J^+)^8 + (J^-)^8\right] + \widetilde{b}\left[(J^+)^4 + (J^-)^4\right] - \widetilde{c}(J_z)^2 \quad \text{(A.1)}$$

Acting in the space $|0\rangle$, $\frac{1}{\sqrt{2}}(|4\rangle + |-4\rangle)$, $\frac{1}{\sqrt{2}}(|4\rangle - |-4\rangle)$ it is represented by the matrix

$$\begin{pmatrix} 0 & b & 0 \\ b & a-c & 0 \\ 0 & 0 & -a-c \end{pmatrix}, \tag{A.2}$$

where $a = 40320\widetilde{a}$, $c = 16\widetilde{c}$, $b = \sqrt{80640}\,\widetilde{b}$.

This Hamiltonian is fully consistent with the crystal field symmetry, and gives the DMFT level sequence in the parameter range $(\sqrt{c^2+2b^2}-c)/2 < a < c$. This sequence of levels is driven by the dynamic hybridization of the U-atom with the Si orbitals pointing towards U, physics which is contained in the LDA + DMFT calculations. Note that the Kondo effect (dynamical hybridization Δ) reverses the order of the LDA crystal field levels.

Notice, however, that our effective Hamiltonian and our Landau-Ginzburg theory is quite general and would apply to any sequence of two low-lying singlets (one even and the other odd under inversion along the two crystalline axis).

REFERENCES

[1] Tripathi V., Chandra P. and Coleman P., *Nat. Phys.*, **3** (2007) 78.
[2] Haule K. and Kotliar G., *Nat. Phys.*, **5** (2009) 796.
[3] Shah N., Chandra P., Coleman P. and Mydosh J. A., *Phys. Rev. B*, **61** (2000) 564.
[4] Mineev V. P. and Zhitomirsky M. E., *Phys. Rev. B*, **72** (2005) 014432.
[5] Baek S.-H., Graf M. J., Balatsky A. V., Bauer E. D., Cooley J. C., Smith J. L. and Curro N. J., arXiv:0906.3040.
[6] Janik J. A. *et al.*, *J. Phys.: Condens. Matter*, **21** (2009) 192202.
[7] Fukuda R., Komachiya M., Yokojima S., Suzuki Y., Okumura K. and Inagaki T., *Prog. Theor. Phys. Suppl.*, **121** (1995) 1.
[8] Broholm C., Kjems J. K., Buyers W. J. L., Matthews P., Palstra T. T. M., Menovsky A. A. and Mydosh J. A., *Phys. Rev. Lett.*, **58** (1987) 1467.
[9] Broholm C., Lin H., Matthews P. T., Mason T. E., Buyers W. J. L., Collins M. F., Menovsky A. A., Mydosh J. A. and Kjems J. K., *Phys. Rev. B*, **43** (1991) 12809.
[10] Villaume A., Bourdarot F., Hassinger E., Raymond S., Taufour V., Aoki D. and Flouquet J., *Phys. Rev. B*, **78** (2008) 012504.
[11] Aoki D., Bourdarot F., Hassinger E., Knebel G., Miyake A., Raymond S., Taufour V. and Flouquet J., *J. Phys. Soc. Jpn.*, **78** (2009) 053701.
[12] Pfleiderer C., Mydosh J. A. and Vojta M., *Phys. Rev. B*, **74** (2006) 104412.
[13] van Dijk N. H., Bourdarot F., Klaasse J. C. P., Hagmusa I. H., Brück E. and Menovsky A. A., *Phys. Rev. B*, **56** (1997) 14493.
[14] Hassinger E., Knebel G., Izawa K., Lejay P., Salce B. and Flouquet J., *Phys. Rev. B*, **77** (2008) 115117.
[15] Yokoyama M., Amitsuka H., Tenya K., Watanabe K., Kawarazaki S., Yoshizawa H. and Mydosh J. A., *Phys. Rev. B*, **72** (2005) 214419.
[16] Wolf B., Sixl W., Graf R., Finsterbusch D., Bruls G., Lauthi B., Knetsch E. A., Menovsky A. A. and Mydosh J. A., *J. Low Temp. Phys.*, **94** (1994) 307.
[17] Kiss A. and Fazekas P., *Phys. Rev. B*, **71** (2005) 054415.
[18] Yokoyama M., Amitsuka H., Itoh S., Kawasaki I., Tenya K. and Yoshizawa H., *J. Phys. Soc. Jpn.*, **73** (2004) 545.
[19] Millis A. J., *Phys. Rev. B*, **48** (7183) 1993.
[20] Motoyama G., Yokoyama N., Sumiyama A. and Oda Y., *J. Phys. Soc. Jpn.*, **77** (2008) 123710.
[21] Jo Y. J., Balicas L., Capan C., Behnia K., Lejay P., Flouquet J., Mydosh J. A. and Schlottmann P., *Phys. Rev. Lett*, **98** (2007) 166404.
[22] Hassinger E., Derr J., Levallois J., Aoki D., Behnia K., Bourdarot F., Knebel G., Proust C. and Flouquet J., *J. Phys. Soc. Jpn., Suppl. A*, **77** (2008) 172.
[23] Takimoto T., *J. Phys. Soc. Jpn.*, **75** (2006) 034714.
[24] Nieuwenhuys G. J., *Phys. Rev. B*, **35** (1987) 5620.
[25] Amoretti G., Balise A. and Mulak J., *J. Magn. & Magn. Mater.*, **42** (1984) 65.